

## PHOTOMETRIC VARIABILITY IN THE HR-DIAGRAM

L. Eyer, M. Grenon

Geneva Observatory, CH-1290 Sauverny, Switzerland

### ABSTRACT

The HIPPARCOS satellite has detected systematically variable stars when the amplitudes exceed a magnitude dependent threshold, as small as a few mmag for bright stars. The published data about variable stars result from the work of two groups at the Geneva Observatory and at the Royal Greenwich Observatory. It contains information about periodic variables (extrema, periods and epochs) and about "unsolved" variables (amplitudes). Here, a more general description of the HR-diagram is made in terms of stability, microvariability, variability, and variation time scales. A particular emphasis is put on the limits of stability areas and their signification.

Key words: Variable Stars, photometry, Hipparcos.

### 1. INTRODUCTION

HIPPARCOS furnished more than 13 million photometric measurements for 118 204 stars, that is a mean of 110 Hp magnitudes per star over a time span of 3.3 years. However the number of these measurements may vary strongly from one star to another as well as the time sampling coverage over the observed period. The Hp passband is wide, it extends from 320 nm up to 850 nm, with a mean wavelength of 537 nm, close to that Johnson V (556 nm).

Before HIPPARCOS, the systematic searches for variable stars were done photographically, with a minimum detectable amplitude of around  $0.3 m_{pg}$ .

With the advance of technologies photoelectric detectors and CCD cameras became available. The precision achieved reached few hundreds to few millimagnitudes. But there was no global survey of the whole sky and stars found photoelectrically as variable were discovered accidentally or using spectral criteria. However, some general studies were done on large data collections, for example with the Geneva photometric data (Grenon 1993).

After the analysis of the main mission data, two catalogues and three atlases were produced : the Catalogues of Periodic stars and of Unsolved stars, the Atlas of Periodic stars (folded curves), the Atlas of Light Curves of stars in common with AAVSO, and

the Atlas of Unsolved variables (light curves) which contains a selection of well defined curves. Many new variables were discovered and many others have a better definition of their behaviour.

Here, we attempt a more global approach, since HIPPARCOS allows a general description throughout the HR-diagram of stellar stability and variability. The HIC (Hipparcos Input Catalogue, cf. Turon et al. 1992) was built in order to be a complete survey up to the magnitude  $V < 7.9 + 1.1 \sin(b)$  for stars earlier than G5 and  $V < 7.3 + 1.1 \sin(b)$  for stars later than G5, where  $b$  is the galactic latitude. The fainter stars in the program emerged as a selection of proposed stars. Altogether, this gives a large sample on which statistical behaviours can be studied.

The choice was made to represent the HR-Diagram in a non conventional way. That is to express it with the spectral classification. In the abscissa is displayed the spectral type and in the ordinate the luminosity class. The spectral types were taken from the HIP catalogue (47% of the stars have a complete information of spectral classification). This for several reasons. First, we didn't have the parallaxes. Second, the spectral classification offers a natural way to bin stars. Third, it is reddening free. Fourth, intrinsically very luminous stars with reliable parallaxes are rare.

### 2. NON VARIABLE STARS

The precision on an individual Hp magnitude depends strongly on the magnitude itself, although more observing time was allocated for fainter stars. Thus the threshold to detect stars as variable is increasing with the magnitude, mainly a result of photon statistics and sky background. Constant stars are then defined as stars not detected as variable at a certain level, magnitude dependent.

The detection threshold limit for stars with a mean number of measurement  $N_m = 110$  is given in Figure 1. If in the shaded area, a star must be considered as of unknown status, constant or variable with a peak-to-peak amplitude  $< A_{lim}$ . If located in the zone between the solid and dotted lines, it is defined as a suspected variable and as a confirmed variable if above the dotted line with  $\leq 0.1$  % probability to be constant.

Six different tests were used to detect variables, with different sensitivities to light-curve features. The mathematical expression for the limiting amplitude is given in Section 4.

For constant stars, i.e. with  $A < 0.02$  mag or so, the standard error on the median magnitude may be extremely small (less than 1 mmag). The set of constant stars provides a high accuracy photometric reference system.

Nevertheless the very high precision on  $Hp_{\text{med}}$  is degraded when  $Hp$  magnitudes are transformed into Johnson V or Strömgen  $y$  magnitude because of residuals on transformation equations, function of the star temperature, gravity, reddening or even metallicity.

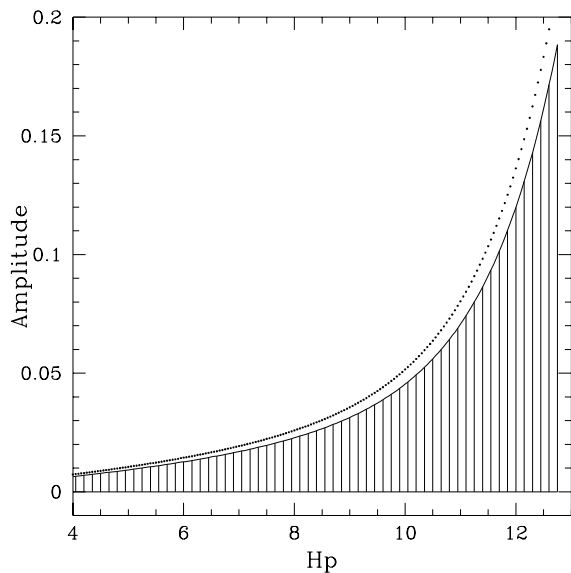


Figure 1. Limits between constant, suspected variable, and variable stars for stars with a mean number of observations.

The confirmation of the variability character from HIPPARCOS time series requires careful examination. Outliers due to light contamination, image overlapping, mispointing may mimic flares or eclipses. Trends due to incorrect colour used in the reduction mimic secular changes as observed for some Be stars. As a result of the data analysis, most spurious events are flagged in the epoch photometry.

### 3. PERIODIC VARIABLES

When the ratio of the expected amplitude over the noise was above a threshold tuned to leave less than 5% of spurious detections as variable (Eyer et al. 1994), a search for periodicity was done. Several methods were used depending on the variability type (van Leeuwen 1997). Once the period was found a curve fitting process was applied to produce quantities as  $Hp_{\text{min}}$ ,  $Hp_{\text{max}}$ , the amplitude, the epochs and the errors on these parameters.

The applied procedure provides the main mode, in case of pulsation, whereas many stars as  $\delta$  Scuti or SPB (Slowly Pulsating B stars) show a complex power spectrum of oscillation.

The peculiar time sampling by HIPPARCOS produces quite easily spurious short periods. In case of doubt, the period was tested for its robustness. All solutions produced by both teams were carefully compared.

#### 3.1. Period distribution in the HR-diagram

In order to investigate the intrinsic properties of single stars, the confirmed or suspected eclipsing binaries were removed from the sample. Spectroscopic binaries may still contaminate the sample, namely in the area of G0-G5 III-IV stars.

For all spectral types a broad period luminosity relation exists (see Figure 2), the high luminosity stars having the longest periods.

Outside the main stability areas, we observe three main instability zones. That of early type stars, shows the shortest periods for  $\beta$  Cepheids stars in the luminosity range class II-III to IV. Late B and early A main sequence stars show periods around 1 day (SPB, Bp).

Around the classical instability strip, the dichotomy known for RR Lyrae stars, i.e. RRC and RRab is also found for population I stars.

F type subgiants  $< F1$  show  $P < 0.2$  day and of about 1 day if near the red edge of the instability strip. Both G and early K dwarfs show periods within 2 to 10 days, when the variability is rotationally induced.

The period increase with luminosity and with decreasing temperature is very conspicuous for late K and M giants and supergiants.

Because of abundance effect both on the luminosity class and on the spectral type, population II stars as RR Lyrae and RV Tau are not considered.

Short periods (2-5 days) are present for hot supergiants, these modes are possibly superimposed on longer period variations. A typical case is HIP 67261 with an oscillation periods of around 4 days.

### 4. AMPLITUDE VARIABILITY LEVEL

When the methods fail to detect any periodic signal, the star is put in the Catalogue of Unsolved variables. This doesn't mean necessarily that the star is not periodic. We might have missed the period (e.g. HIP 29055) or some minima for eclipsing binaries due to the peculiar sampling, or the periodic behaviour is too complex to be described with the present data set (e.g. multiperiodic variables). In most cases, the variations are indeed aperiodic as it can be seen in the Atlas of light curves of Unsolved variables (Grenon 1997).

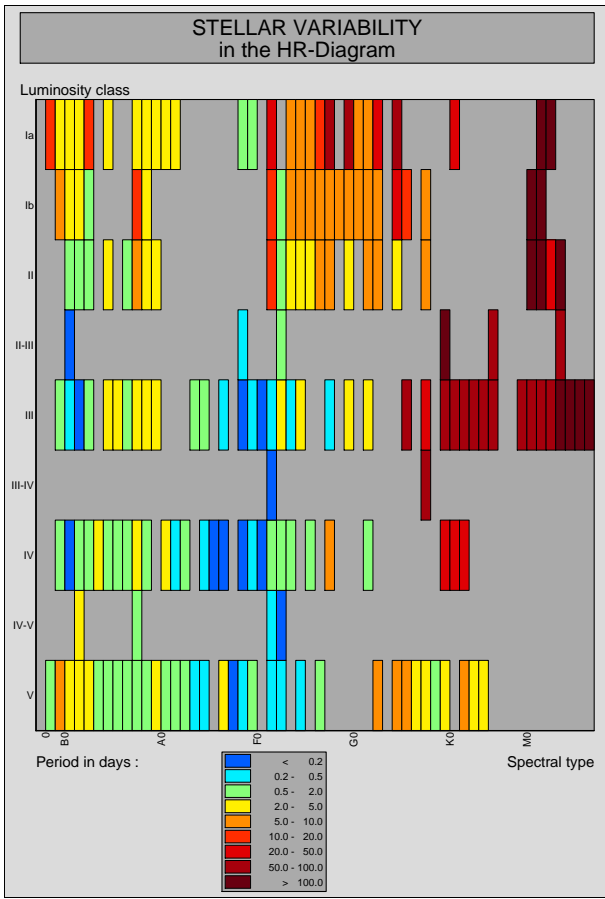


Figure 2. HR-diagram labeled in periods

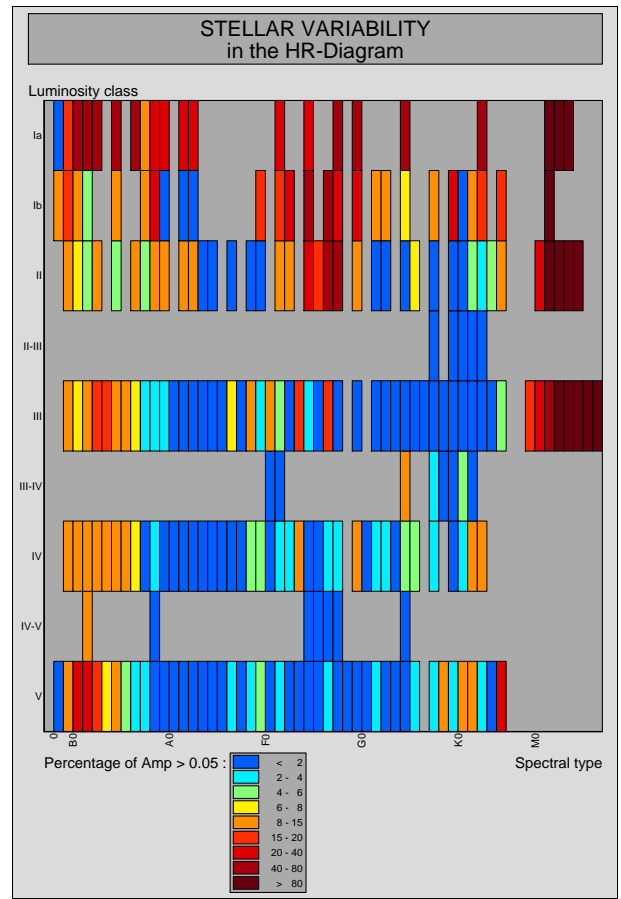


Figure 4. HR-diagram labeled in fraction of variables

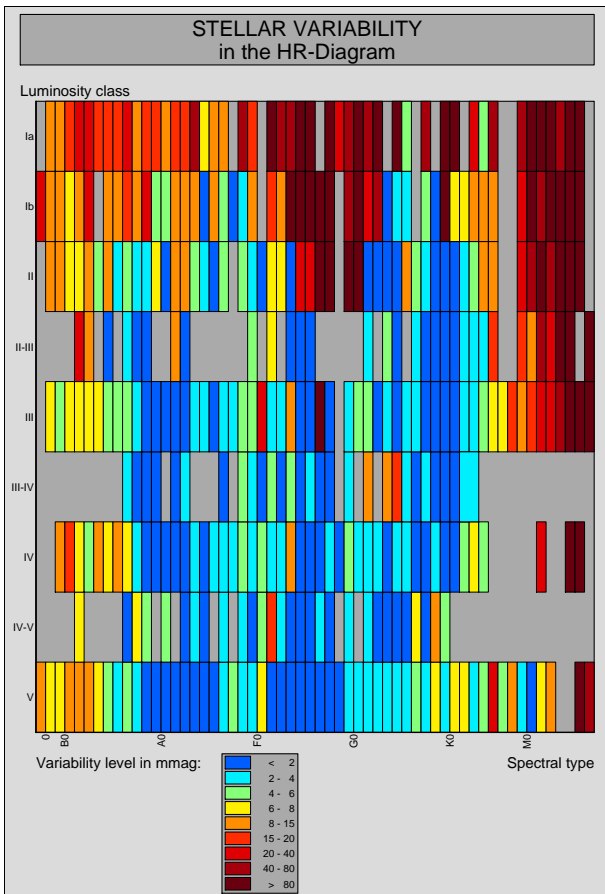


Figure 3. HR-diagram labeled in mean intrinsic scatter

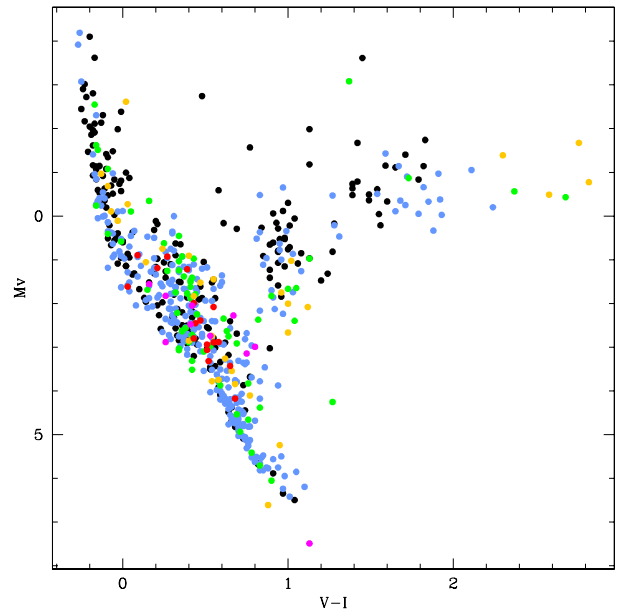


Figure 5. The  $M_v/(V - I)$  diagram for variable stars in the south galactic cap. Symbol colours : black dots :  $A < 0.02$  mag; blue :  $A = 0.02 - 0.05$ ; green :  $A = 0.05 - 0.10$ ; yellow :  $A = 0.10 - 0.25$ ; red :  $A > 0.25$ .

In order to characterize quantitatively the unsolved variables, in addition to their light curves, we defined their intrinsic amplitudes, i.e. their peak-to-peak amplitudes corrected for photon and reduction noises.

The estimated scatter due to photon and reduction noises,  $\epsilon_{\text{int}}$  is subtracted quadratically from the observed scatter  $\sigma_{\text{data}}^2$ . If the variations were sine curves, the amplitude  $A$  would be equal to  $2\sqrt{2}\sigma_{\text{int}}$ , the intrinsic scatter. A correction, function of the asymmetry  $s_3$ , allows to estimate correctly the amplitude even in case of very asymmetric light curves as for EB type variables. The coefficients in the formula given below were tuned, using  $s_3$  and the amplitude obtained from periodic variables with well defined curves fitting. The comparison between the amplitude estimator  $A$  and the true peak-to-peak amplitude  $H p_{\text{min}} - H p_{\text{max}}$  is given in Figure 6. It should be noticed that for small amplitudes the two amplitude estimators converge, with the differences that  $A$  may represent the combination of several modes in case of multiperiodicity, whereas  $H p_{\text{min}} - H p_{\text{max}}$  is the amplitude of the main mode.

The formulae used in the definition of amplitudes are :

$$\sigma_{\text{int}}^2 = \sigma_{\text{data}}^2 - \epsilon_{\text{int}}^2$$

$$A = 2\sqrt{2}\sigma_{\text{int}}\left(2.56 - \frac{1}{0.64s_3^2}\right)$$

$$A_{\text{lim}} = 2\sqrt{2}\epsilon_{\text{int}}\left(\frac{0.18}{(0.003 N_m + 0.5)^2} + 0.43\right)$$

where  $N_m$  is the number of measurements used.

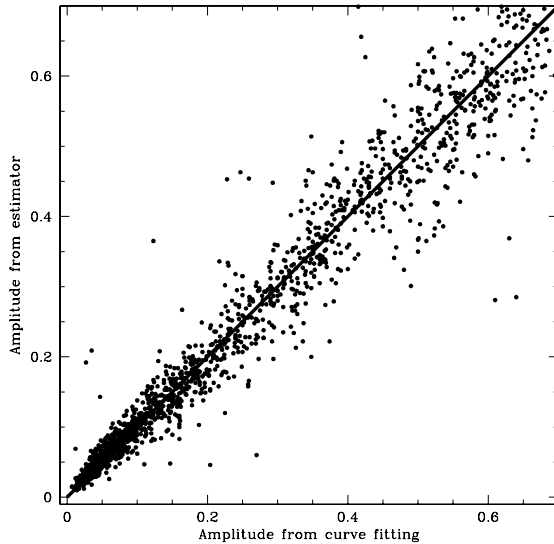


Figure 6. Comparison between the estimated amplitudes and the amplitudes from the catalogue of periodic variables

Due to statistical uncertainties,  $\sigma_{\text{int}}^2$  may be negative. This quantity may nevertheless be used with its sign where mean levels of variability are considered in bin of spectral type and luminosity class.

#### 4.1. Mean intrinsic scatter

The mean intrinsic scatter  $\langle \sigma_{\text{int}} \rangle$  computed from all stars, constant, microvariable and variable is indicative of the variability level across the HR-diagram. A robust estimator of  $\langle \sigma_{\text{int}} \rangle$  is given in Figure 3 for bin of spectral subtype and luminosity class.

Highly stable areas exist on both sides of the classical instability strip extending from F0V to F8II and above. The blue domain is narrowing towards high luminosity. B8-A3 IV and V stars appear to be the most stable whereas early B type stars are nearly all variable. We notice the shift towards lower  $T_{\text{eff}}$  of unstable B subgiants with respect to dwarfs.

The stable domain at the right of the instability strip is contaminated by stars showing probably composite spectra as the G0-G2 III, G2-G5 III-IV for which the variability is non intrinsic. G8II to G8V stars are photometrically the most stable.

With the development of activity and star spots the variability increases from G8 to M2 dwarfs.

Main sequence stars in the instability strip are mostly microvariable with  $\langle \sigma_{\text{int}} \rangle$  up to 6-8 mmag.

The amplitude-luminosity relation is conspicuous for late K and M giants and supergiants as well as the amplitude-temperature relation for M giants, the latest showing the largest intrinsic scatter.

#### 4.2. Amplitudes above 0.05 mag

An other way to characterize the distribution of the variability is through the percentage of variables with amplitudes exceeding a given threshold. The statistics has to be performed with stars having  $A_{\text{lim}}$  less or equal to the selected threshold. A very clear delimitation of variability area is found when the threshold is set to 0.05 mag, see Figure 4. Nearly 50% of B1-2 V stars, 15-20% of B3-B4 III have  $A > 0.05$  mag; they define precisely the instability strip for B stars. The general structure of this diagram is similar to that of Figure 3 with the difference that in some area almost all stars are stable at the 0.05 mag level whereas in other they are nearly all variable, namely the M giants and the Ia supergiants.

#### 4.3. The distribution of amplitudes

The mean amplitude or the fraction of stars above a threshold are crude estimators of the amplitude distribution, and they may be misleading if several modes or variability types are present in a given area of the HR-diagram.

In well populated areas the distribution of amplitudes may be described. It is the case for most of the main sequence, the blue giants and the red giants domains. As an example we give (see Figure 7) the case of the class III M giants, of type M0, M3 and M4 with corresponding temperature from 3800 to 3300° K.

The distributions of red giants amplitudes are unimodal with their modes as well as their spread getting

larger when the temperature gets lower. Furthermore there is a minimum amplitude which is increasing with decreasing temperature. At M4 the minimum amplitude is around 0.04 mag.

## ACKNOWLEDGMENTS

We would like to thank warmly Luc Weber for his efficient help for the production of the colour diagrams.

## REFERENCES

- Eyer, L., Grenon, M., Falin, J.-L., Froeschle, M., Mignard, F., 1994, *Solar Physics* 152, 91-96  
 Grenon, M. 1993, *Astron. Soc. Pacific. Conf. Series* 40, 693  
 Grenon, M., et al., 1997, *ESA SP-1200*, volume 12  
 Turon, C., 1992, *ESA SP-1136*, volume 1-7  
 van Leeuwen, F., 1997, *This meeting*

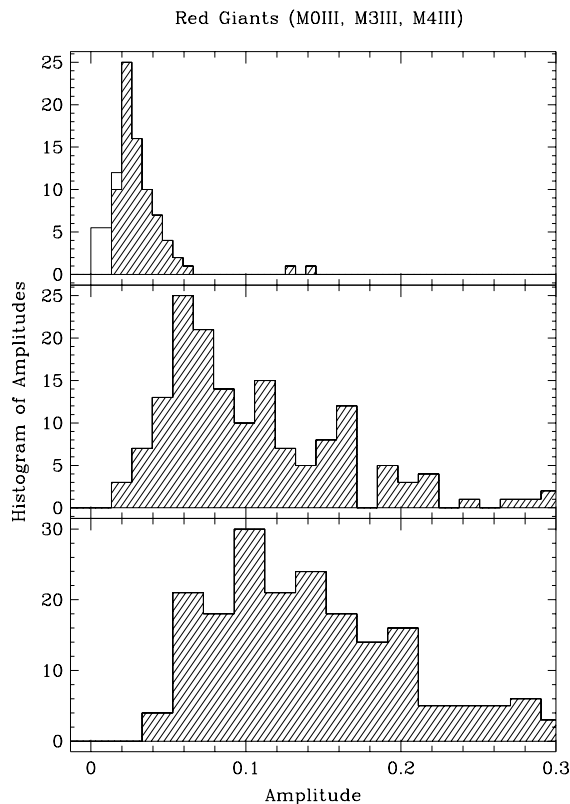


Figure 7. Distribution of amplitudes of *M* giants.

### 4.4. Variability in The $M_v/(V - I)$ plane

For intermediate to low luminosity stars, parallaxes may be used to build the HR-diagram in terms of absolute magnitude  $M_v$  and  $(V - I)$ , see Figure 5. Among 21 657 stars at South Galactic Cap ( $b < -40^\circ$ ) 4824 stars have  $\sigma_{M_v} < 0.2$  and among them 627 show significant amplitudes.

Microvariables,  $A < 0.02$ , are found mainly in the upper main-sequence,  $(V - I) < 0.0$ , in the clump of red giants in core He-burning phase and in the adjacent giant branch. Red subgiants show larger amplitudes. The zone around  $(V - I) = 0.0$  in the main sequence is nearly depleted from variables.

The highest density of variables with  $A = 0.05 - 0.10$  is found for subgiants and dwarfs in the  $(V - I)$  range 0.30-0.45.

Larger amplitude variables are associated to the classical instability strip. They are concentrated at both edges of the Böhm-Vitense gap at  $(V - I) = 0.50$ .